Supplementary Information of "Diagnosing the sensitivity of grounding line flux to changes in sub-ice shelf melting"

Tong Zhang[1], Stephen Price[1], Matthew Hoffman[1], Mauro Perego[2], and Xylar Asay-Davis[1]

[1]Fluid Dynamics and Solid Mechanics Group, Los Alamos National Laboratory, Los Alamos, NM, 87545, USA
[2]Center for Computing Research, Sandia National Laboratories, Albuquerque, NM, 87185, USA

Correspondence: T. Zhang (tzhang@lanl.gov), S. Price (sprice@lanl.gov)

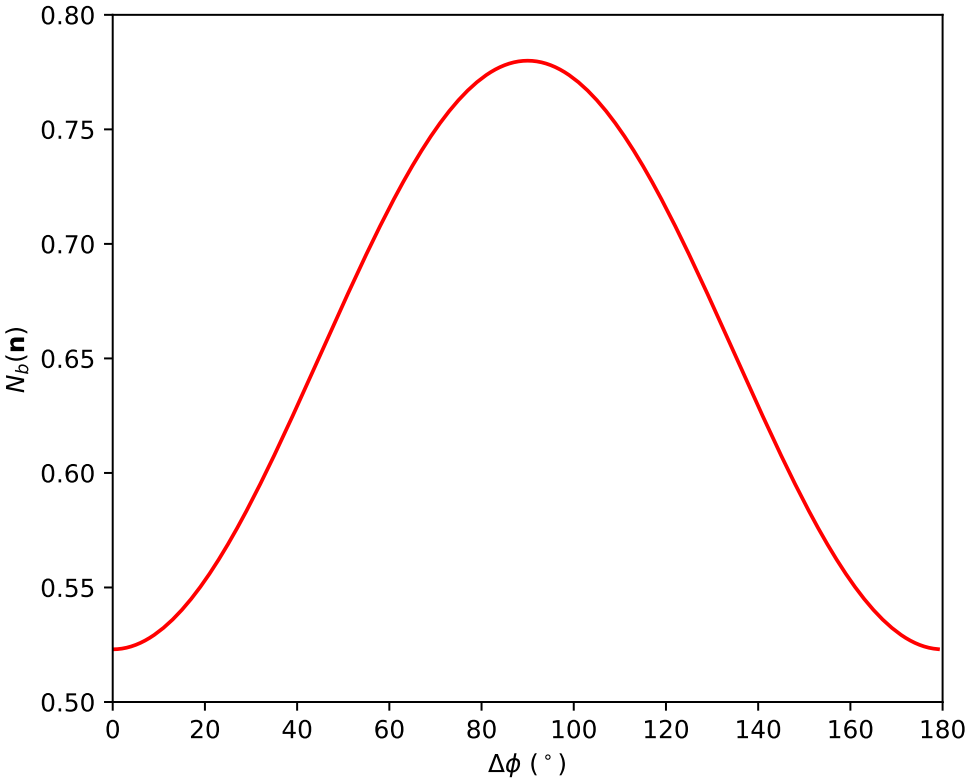

Figure S1. N_b values rotated counterclockwise by $\Delta\phi$ degrees relative to the direction corresponding to σ_{p1} ($\mathbf{n}_{p1}$)

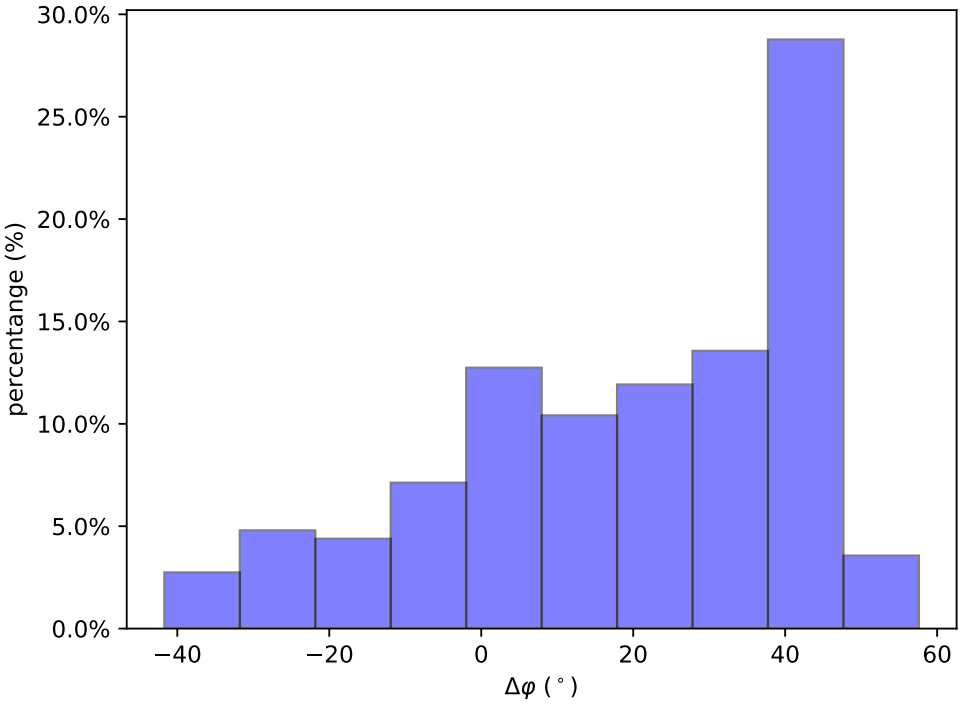

Figure S2. Histograms showing the angular difference between $\mathbf{n}_{p1}$ and $\mathbf{n}_f$. Points analyzed are those from Fig. 4.

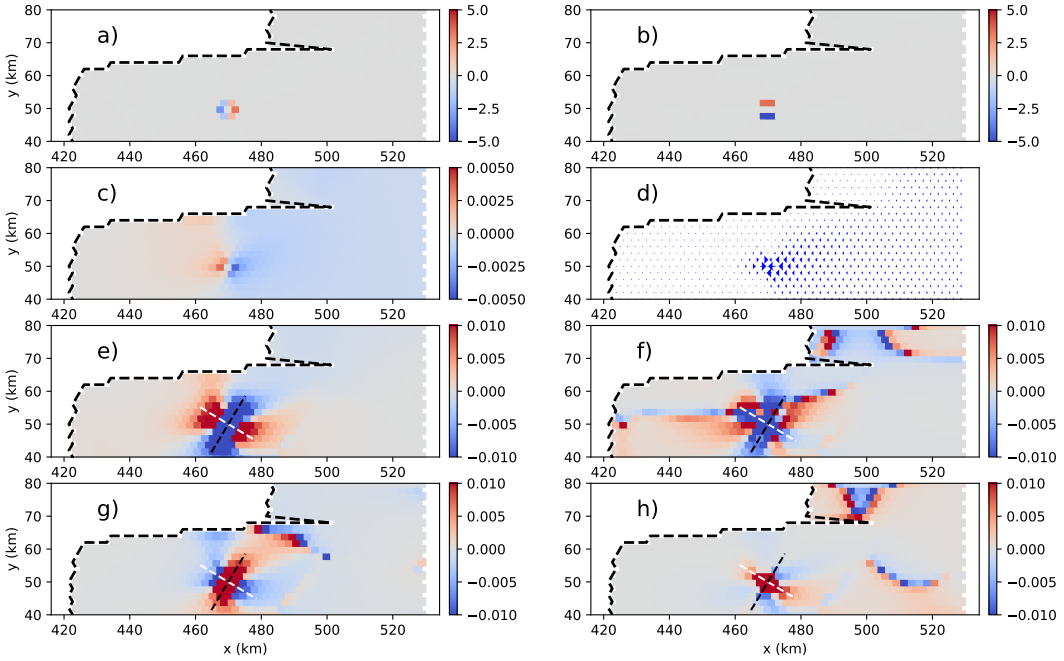

Figure S3. An example of the local change (ratio, in %) in (a) the ice thickness gradient in x, (b) ice thickness gradient in y, (c) ice speed, (d) ice velocity (relative), (e, f) principal strain rates, and (g, h) buttressing number following a local perturbation to the ice shelf thickness. In (e) and (g), changes (colors) are associated with the $\mathbf{n}_{p1}$ direction and for (f) and (h) changes are associated with the $\mathbf{n}_{p2}$ direction. The white- and black-dashed lines show the direction of $\mathbf{n}_{p1}$ and $\mathbf{n}_{p2}$ at the perturbation location, respectively.

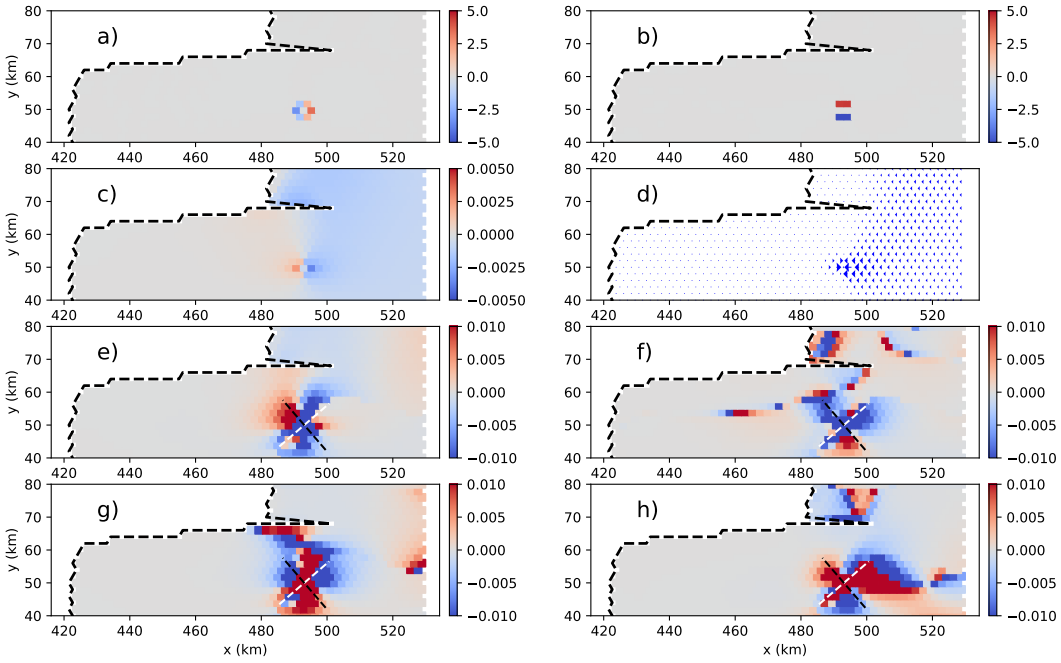

Figure S4. An example of the local change (ratio, in %) in (a) the ice thickness gradient in x, (b) ice thickness gradient in y, (c) ice speed, (d) ice velocity (relative), (e, f) principal strain rates, and (g, h) buttressing number following a local perturbation to the ice shelf thickness. In (e) and (g), changes (colors) are associated with the $\mathbf{n}_{p1}$ direction and for (f) and (h) changes are associated with the $\mathbf{n}_{p2}$ direction. The white- and black-dashed lines show the direction of $\mathbf{n}_{p1}$ and $\mathbf{n}_{p2}$ at the perturbation location, respectively.

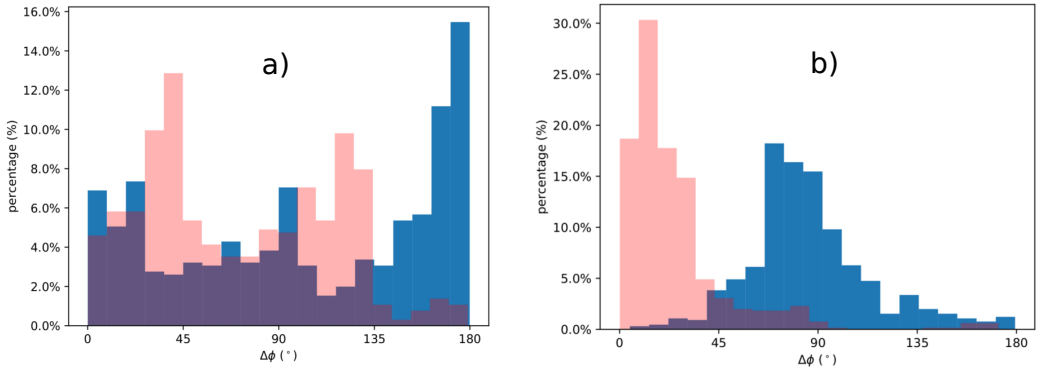

Figure S5. Histograms for the maximum (red) and minimum (blue) percent speed increases in grid cells adjacent to a thickness perturbation on the Larsen C ice shelf, plotted as a function of angular distance with respect to (a) $\mathbf{n}_{p1}$ and (b) $\mathbf{n}_f$.

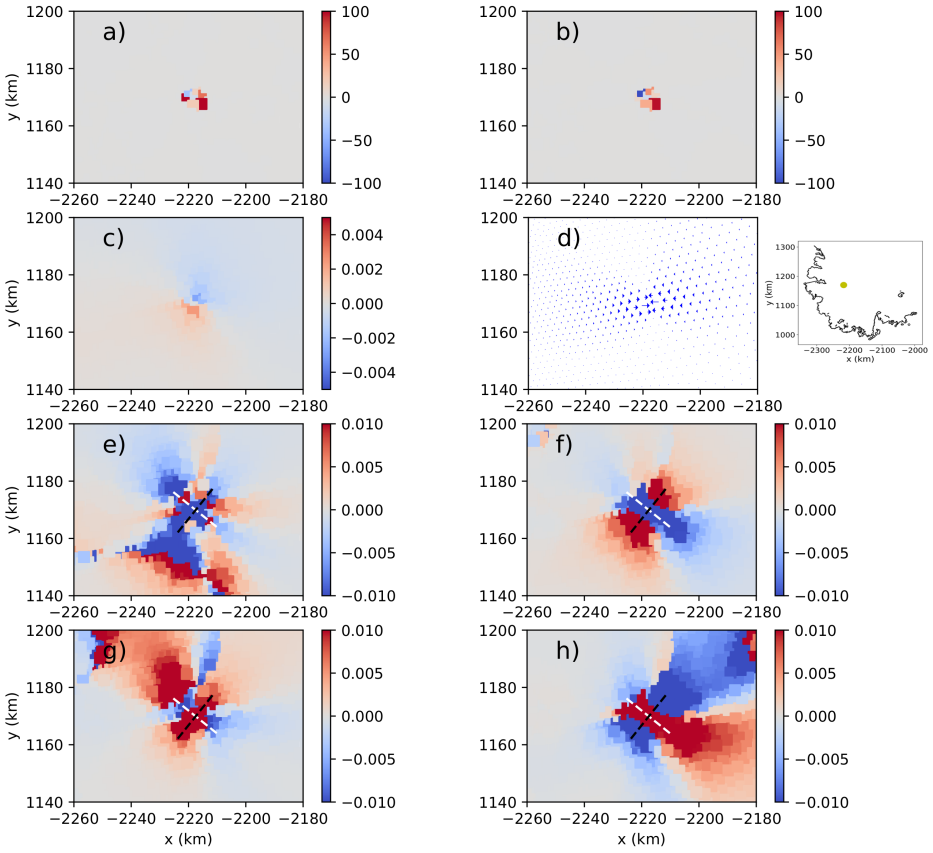

Figure S6. An example of the local change (ratio, in %) in (a) the ice thickness gradient in x, (b) ice thickness gradient in y, (c) ice speed, (d) ice velocity (relative), (e, f) principal strain rates, and (g, h) buttressing number following a local perturbation to the ice shelf thickness. In (e) and (g), changes (colors) are associated with the $\mathbf{n}_{p1}$ direction and for (f) and (h) changes are associated with the $\mathbf{n}_{p2}$ direction. The white- and black-dashed lines show the direction of $\mathbf{n}_{p1}$ and $\mathbf{n}_{p2}$ at the perturbation location, respectively.

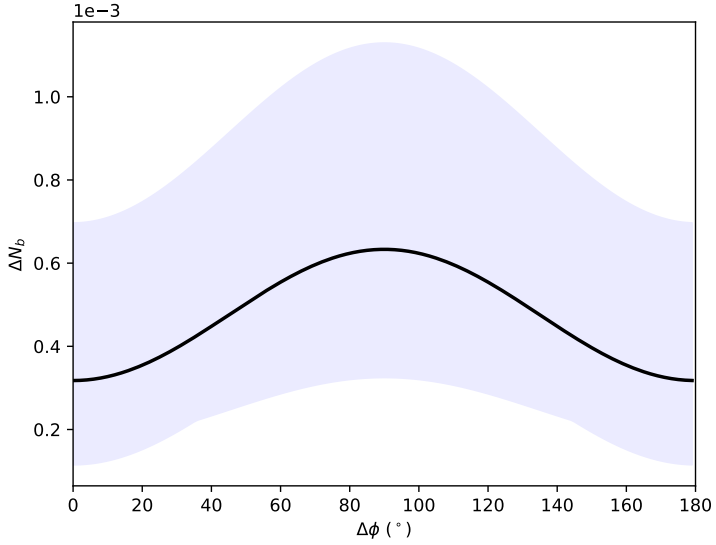

Figure S7. The change in buttressing number ΔN_b at the neighboring cells with maximum ice speed increase for each perturbation point in the inset of Fig. 14 that are $>$ 50 km away from the grounding line and the calving front of the Larsen C shelf. Changes in buttressing are calculated along the direction $\Delta\phi$, rotated counterclockwise relative to the $\mathbf{n}_{p1}$ direction.

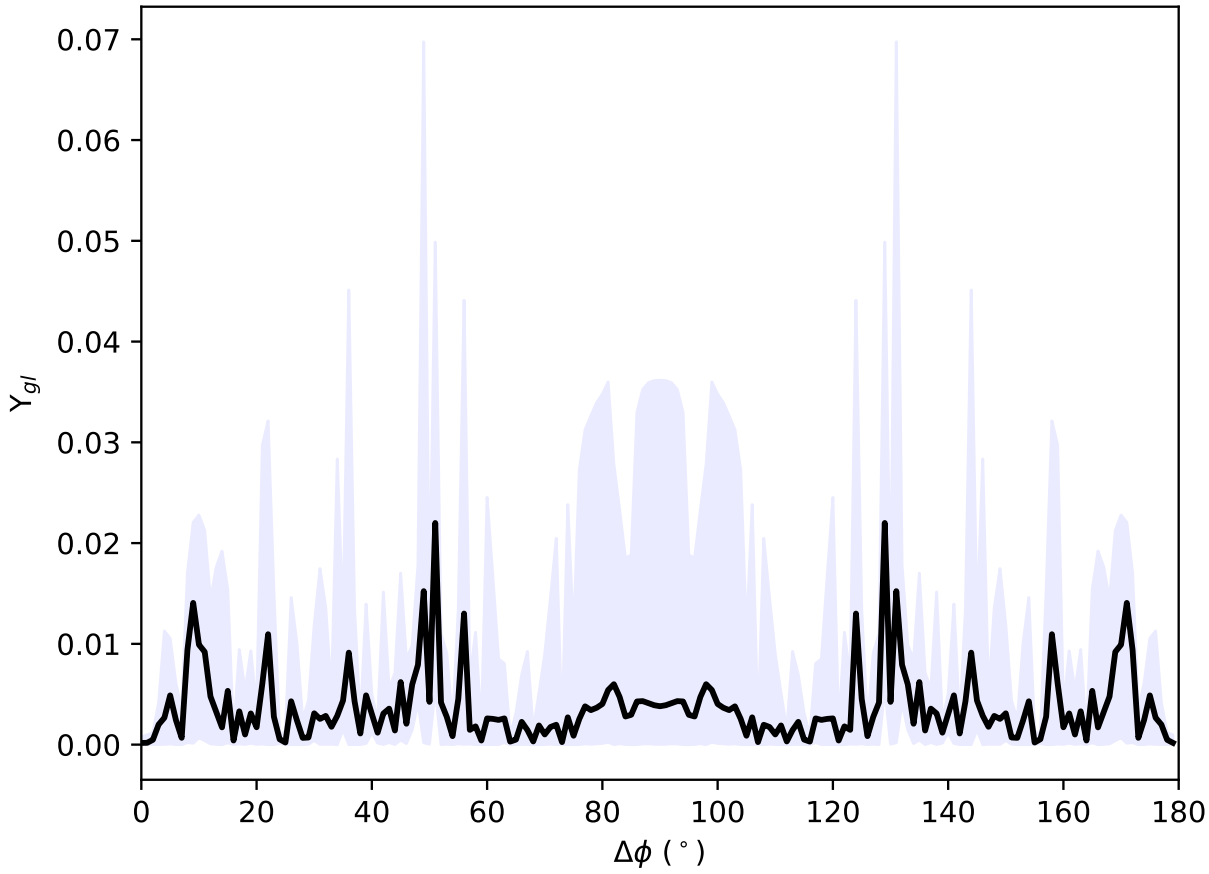

Figure S8. Correlation between the change in normal stress and the change in ice surface speed along grounding line (i.e., Υ_{gl} from Eq. 12) for Larsen C experiments. The horizontal axis shows how Υ_{gl} varies as a function of the direction $\mathbf{n}$ used to define the normal stress, rotated counterclockwise from $\mathbf{n}_{p1}$. The blue shaded area is the range for all perturbation experiments (same as in Fig. 5a) and the thick black curve is their mean value.